Li12C60: A lithium clusters intercalated fulleride

9 AUTHORS, INCLUDING:

Daniele Pontiroli
Università degli studi di Parma
49 PUBLICATIONS   **357** CITATIONS

SEE PROFILE

Mattia Gaboardi
Università degli studi di Parma
20 PUBLICATIONS   **96** CITATIONS

SEE PROFILE

Pietro Galinetto
University of Pavia
126 PUBLICATIONS   **855** CITATIONS

SEE PROFILE

Chiara Milanese
University of Pavia
110 PUBLICATIONS   **902** CITATIONS

SEE PROFILE

Li$_{12}$C$_{60}$: A lithium clusters intercalated fulleride

Fabio Giglio [a], Daniele Pontiroli [a,b], Mattia Gaboardi [a], Matteo Aramini [a], Chiara Cavallari [a,c], Michela Brunelli [c], Pietro Galinetto [d], Chiara Milanese [e], Mauro Riccò [a,*]

[a] Dipartimento di Fisica e Scienze della Terra, Università degli Studi di Parma, Via G. P. Usberti 7/a, 43124 Parma, Italy
[b] Laboratorio di Micro e Submicro Tecnologie abilitanti dell'Emilia Romagna (MIST.E-R), Via P. Gobetti 101, 40129 Bologna, Italy
[c] Institut Laue Langevin, BP 156, 6 rue Jules Horowitz, 38042 Grenoble Cedex 9, France
[d] Dipartimento di Fisica 'A. Volta', Università di Pavia, Via Bassi 6, 27100 Pavia, Italy
[e] Pavia Hydrogen Lab, Dipartimento di Chimica, Sezione di Chimica Fisica, Università di Pavia, V.le Taramelli 16, 27100 Pavia, Italy

ARTICLE INFO

ABSTRACT

We report the structural analysis of the highly-doped lithium fulleride Li$_{12}$C$_{60}$, performed using low-temperature neutron powder diffraction. Although the main reflections could be initially indexed with a fcc cell, Monte Carlo Simulated Annealing suggests an unusual monoclinic arrangement for the fullerene molecules. In this structure, C$_{60}$ units with the same orientation are alternatively stacked to form layers, thus maximising their sterical crowding. Rietveld refinement allowed to localise Li ions, which are organised in clusters belonging to the pseudo-tetrahedral voids with a non-complete charge transfer as confirmed by Raman spectroscopy.

© 2014 Elsevier B.V. All rights reserved.

1. Introduction

During the past years, alkali and alkali-earth intercalated fullerides were intensely investigated, especially due to their unusual physical properties, such as superconductivity, metal-to-insulator transition, long range magnetism and polymerisation [1–5]. More recently, these systems, in particular light metal (lithium, sodium and magnesium) C$_{60}$ intercalated compounds, have gained renewed interest for energy storage applications, either as novel materials for ion batteries [6–9] or in the field of hydrogen storage [10–13].

Particular is the case of Li$_x$C$_{60}$ systems, where the small size of Li ions with respect to the relatively large free volume of fullerite leads to the formation of a wide family of compounds [14] and the intercalation of up to 28 lithium atoms per fullerene molecule without an evident segregation of the metal was reported [15]. At low doping level ($x < 6$), the negative charge transferred from Li to C$_{60}$, together with the small size of the Li ion, allows the formation of fullerene polymers [16], able to sustain the light metal ion diffusion also at room temperature [7]. On the other hand, at high doping fraction ($x \geqslant 6$), the tendency of Li atoms to partially donate their charge to C$_{60}$ [17] facilitates the formation of clusters inside the fullerene voids [18–20].

Recently, Li fullerides demonstrated to be able to reversibly absorb relatively high amount of hydrogen. A theoretical work predicted that 12 Li atoms can coordinate to the 12 pentagonal faces of the C$_{60}$ molecule, thus preserving its icosahedral symmetry [21]. This 'superfulleroid' configuration is presumed to be stable and to behave as an exceptional hydrogen storage system, capable to adsorb up to 13 wt% H$_2$ with a binding energy favourable for applications, through an enhanced physisorption mechanism [22]. However, it is still an unresolved question whether it is possible or not to stabilize the superfulleroid arrangement in the solid state, the only experimental proof of its formation arising from ionization spectroscopy in gaseous phases [23]. From the experimental point of view, Teprovich et al. explored various stoichiometries for the LiH:C$_{60}$ system and reported up to 5 wt% H$_2$ reversible desorption for samples with 6:1 ratio with an onset temperature of 270 °C [10]. We found the same amount of hydrogen can also be stored in samples with stoichiometry Li$_{12}$C$_{60}$, where the absorption was found to start already below 100 °C (190 bar), namely 200 °C lower than pure C$_{60}$ [12]. In these compounds, the presence of metallic clusters, together with the high charged state of C$_{60}$, turn out to be essential ingredients for the hydrogen absorption mechanism [24], which occurs through the hydrogenation of the fullerene molecule and the formation of the C$_{60}$H$_y$ hydrofullerite [25]. However, for Li$_{12}$C$_{60}$ the complete knowledge of the structure is not complete yet, in spite of its importance to better understand the mechanism of hydrogenation of this compound. In fact, the previous structural investigation on solid Li$_{12}$C$_{60}$ was carried out only on the high temperature fcc phase ($T = 250$ °C) and indicated the formation of Li clusters inside the bigger octahedral voids of the fullerene lattice [26]. On the other hand,

* Corresponding author. Fax: +39 0521905223.
E-mail address: Mauro.Ricco@fis.unipr.it (M. Riccò).

the structure of $Li_{12}C_{60}$ for lower temperatures, where a distortion to a tetragonal phase was supposed, is still unknown.

In this work we present a novel efficient synthesis route for producing polycrystalline $Li_{12}C_{60}$ via solid state reaction promoted by means of high energy ball-milling technique and subsequent annealing. Crystallographic investigation, based on Monte Carlo Simulated Annealing analysis performed on neutron diffraction data collected at 20 K is discussed, which provided a complete structure description of the $Li_{12}C_{60}$ ground state. Complementary characterisation was carried out by means of micro-Raman spectroscopy.

2. Experimental methods

C_{60} powder (MER, 99.9± % purity) was mixed to small pieces of lithium (Sigma–Aldrich, 99% purity) in the stoichiometric ratio 1:12, in order to obtain typical 400–500 mg batches of powder. The grinding process took place in a 10 ml volume agate ball-milling jar containing the sample and 3 agate spheres of 10 mm diameter (Fritsch Mini-Mill Pulverisette 23), which was mechanically shaken at 30 Hz for 60 min (typical milling step takes 10′ followed by 5′ pause, in order to avoid jar overheating). Since the synthesized samples are very air and moisture sensitive, their preparation and handling were performed in an Ar filled glovebox (H_2O and O_2 levels under 1 ppm). The resulting black powder was then pelletized, placed in Ta foil bags, sealed under high vacuum (<10^{-5} mbar) in a Pyrex® vial and subsequently treated in a furnace at 270 °C for 36 h. The final product, in form of powder, was obtained by grinding the treated pellets.

Samples, sealed in 0.7 mm glass capillaries, underwent preliminary X-ray powder diffraction characterisation at room temperature with a Bruker D8 Discover diffractometer, working in Debye Scherrer geometry and equipped with an area detector (GADDS) and a Cu anode (λ = 1.5460 Å). Qualitative X-ray diffraction scans generally take 10–16 h of collecting time in order to obtain a good statistics. Neutron powder diffraction data were collected at the D20 diffractometer at the Institut Laue-Langevin (ILL), Grenoble (France). Neutron scattering measurements (λ = 1.3593 Å) were collected over 5 h on ~400 mg of $Li_{12}C_{60}$ sample, loaded into a sealed vanadium sample holder, then placed in a cryostat at T = 20 K. Low temperature setup was chosen in order to decrease the Debye–Waller damping contribution and to freeze any possible Li and C_{60} molecule dynamics. Neutron powder diffraction data underwent ab-initio structural analysis by using the Reflex module of Materials Studio 6.0 suite (Accelrys Inc.) and the GSAS suite.

Micro-Raman measurements were carried out at room temperature by using a Labram Dilor spectrometer equipped with an Olympus microscope HS BX40. The 632.8 nm light from He–Ne laser was employed as excitation radiation. The samples were sealed in borosilicate glass capillary and tested with a 50× objective and with a laser spot of ~1.2 μm of diameter. The spectral resolution was about 1 cm^{-1}. Neutral filters with different optical density were used to irradiate the samples at different light intensities leading to power density values from 5×10^2 W/cm^2 to 5×10^5 W/cm^2. In order to avoid polymerisation of the C_{60} molecules, the power density was in any case kept at 6×10^4 W/cm^2 using an optical filter with DO = 0.6. A cooled CCD camera was used as a detector and the typical integration times were about 3 min. The phase homogeneity has been verified by mapping the Raman spectra from different regions of the samples.

3. Results and discussion

The laboratory X-ray powder diffraction pattern of $Li_{12}C_{60}$ collected at room temperature (Figure 1a) indicated that the sample is single-phase, since all the peaks can be easily indexed with the fcc cubic cell. No evident segregation of unreacted Li or pure C_{60} was detected.

The pattern decomposition performed with Le Bail method allowed to extract the lattice parameter of the fcc cell (space group Fm$\bar{3}$m), which resulted a = 13.997(4) Å, slightly contracted if compared with the pure C_{60} cubic phase (a = 14.16 Å). The C_{60} intermolecular distance, of ~9.9 Å, is compatible with fullerenes in the monomer state, differently from what observed in the low-doped lithium intercalated fullerides, where fullerenes polymerisation was observed [3]. However, no evident phase transitions were detected in the sample, from X-ray diffraction analysis, on cooling the sample down to 90 K (not shown), suggesting that buckyballs are probably non-rotating already at room temperature, due to the presence of the intercalant phase.

Neutron powder diffraction data collected at 20 K contain much more information, especially at the high-angle region, and allowed us to perform an ab-initio structural investigation. The data were first corrected by subtracting the empty cell signal. At a first stage of the analysis, the contribution of the Li atoms to the structure factors was neglected, since it is much smaller than the C contribution. Due to symmetry analogies with the well-known fcc phase of pristine C_{60}, we chose to use it as starting model of our analysis. Two fcc structural models were initially tested: either the most common merohedrically disordered C_{60} phase (space group: Fm$\bar{3}$m), or a structure in which C_{60} units are ordered (spatial group Fm$\bar{3}$), observed in some intercalated C_{60} compounds [27]. In both cases, Le Bail pattern decomposition provided a good fit of the observed data, but the Rietveld refinement returned indeed a poor agreement, especially in the high angle range of the diffractogram (see Figure 1b and c). We also considered a model analogue to the low temperature ordered C_{60} phase (space group Pa$\bar{3}$) achieving also in this case a low agreement (R_{wp} = 17.5%, see Figure 1d).

These findings suggested that, in $Li_{12}C_{60}$, C_{60} molecules are arranged in a cubic-like close-packed lattice, but with a still unknown orientation, which does not match the tested structures. For this reason, we decided to search the correct arrangement of the carbon backbone with the technique of Monte Carlo Simulated Annealing (MO-SA), which is a powerful tool for the resolution of complex minimisation problems, such as ab-initio structural investigation starting from powder diffraction data.

Our starting model consisted in a cell where the C_{60} centres of mass sit on the nodes of an fcc lattice, but with no symmetry constrains. To obtain this, all symmetry operators were removed in order to get a 'pseudo-cubic' cell ($a = b = c$ = 13.997 Å, $\alpha = \beta = \gamma = 90°$) with P1 space group symmetry. Therefore, during the SA routine, fullerenes were free to explore all the possible rotational and translational degrees of freedom. In order to reduce computational time, at a first step the complexity of the cell was reduced by describing the original fcc lattice, comprising four C_{60} molecules, with a smaller body-centred tetragonal (bct) one, which encloses only two C_{60} units. This was obtained by applying the coordinate transformation:

$$a = a'/\sqrt{2} \qquad c = a'$$

where a' is the fcc cubic original lattice parameter, while a and c are the lattice parameters of the new tetragonal cell. MO-SA cycles performed on this model allowed us to obtain a new molecular position, able to much better describe the high angular region of the neutron pattern data (R_{wp} = 7.8%).

In this new structure, C_{60} centres of mass are still placed in a fcc lattice, but, as a consequence of the presence of two non-equivalent molecules in the cell, they were found in two different orientations, with C_{60} rotated of ~90° around the (001) of the parent cubic axis. Fullerenes displaying the same orientations form
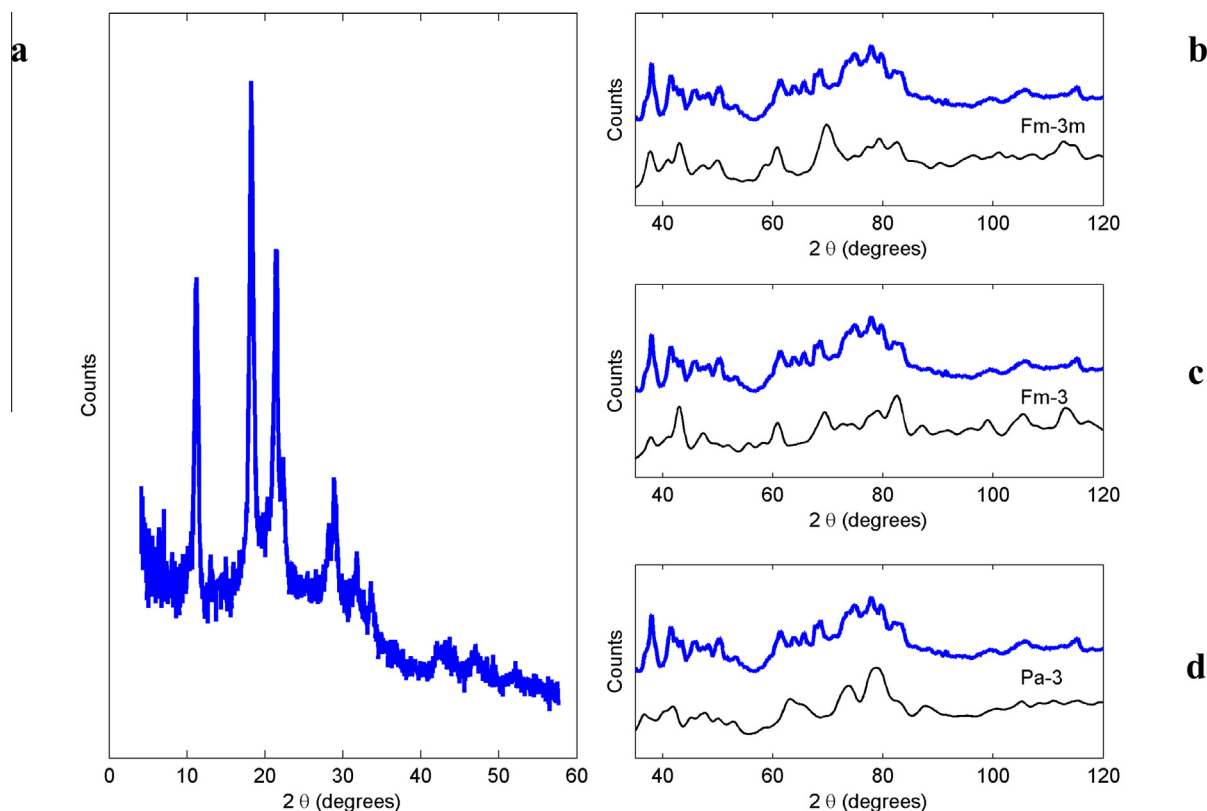
Figure 1. (a) Laboratory X-ray powder diffraction pattern of $Li_{12}C_{60}$ (Cu Kα) collected at room temperature. (b–d) Comparison between the experimental neutron powder diffraction pattern of $Li_{12}C_{60}$ at 20 K (thick solid line) and the diffraction profile (thin solid line) corresponding to C_{60} molecules respectively placed in a *fcc* lattice with merohedral disorder (S.G. Fm$\bar{3}$m), in a *fcc* lattice with ordered arrangement (S.G. Fm$\bar{3}$) and in a primitive cubic lattice observed in the low-temperature C_{60} phase (S.G. Pa$\bar{3}$). During this step the scattering contribution arising from Li was neglected.
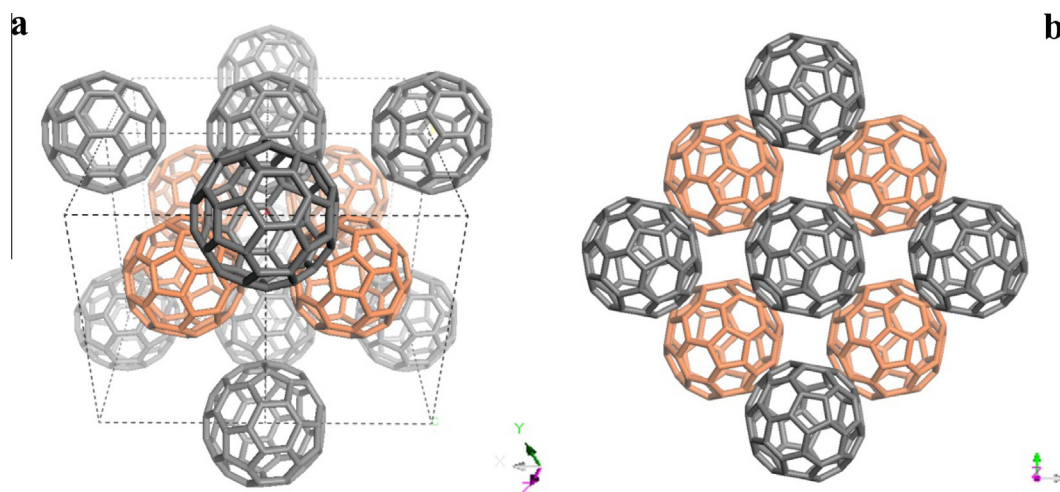

Figure 2. Structural C_{60} molecule arrangement in $Li_{12}C_{60}$ obtained with MO-SA from a symmetry-unrestricted (S.G. P1) starting cell, which mimics the *fcc* molecular arrangement suggested by indexing process. The disposition of fullerenes is described by a monoclinic cell with space group P2$_1$/c. (a) View along the [1 0 1] direction of the monoclinic cell (edges evidenced with dotted line) shows that fullerenes with the same orientation form layers, alternatively stacked along [0 0 1] parent cubic direction. (b) View along [0 0 1] direction.

layers, alternatively stacked along the same direction (see Figure 2a and b). Due to this new arrangement, the symmetry of this structure resulted lowered and can be described in the monoclinic P2$_1$/c space group. In order to check if the small size of our starting model limited the search to the possible structural solutions, we tackled the MO-SA analysis also on the bigger cell, comprising four non-equivalent C_{60} molecules. The result obtained was in good

agreement with the proposed model, thus validating the previously obtained structure.

Rietveld refinement against the neutron powder diffraction data was performed by considering the structure obtained with MO-SA as the starting model (Figure 4b). During the refinement, either the lattice parameters or the atomic positions were let to vary, however treating C_{60} as a rigid body. Cell parameters of the

refined P2$_1$/n monoclinic cell (the second cell choice of the suggested P2$_1$/c space group was used for an easier structure representation) resulted in: $a = 9.888(9)$ Å, $b = 9.901(8)$ Å, $c = 14.290(8)$ Å, $\beta = 89.51(6)°$, ($R_{wp} = 7.36\%$, $R_{F2} = 4.72\%$). The refined cell parameters suggested the presence of a weak expansion of the lattice along the [0 1] direction of the derived cubic structure, namely in direction orthogonal to layers formed by equally oriented C$_{60}$ units (~14.3 Å along the [0 0 1] direction against ~14 Å along the [1 0 0] one), indicating that the structure is weakly anisotropic. The volume per C$_{60}$ turn out to be of 699.5(5) Å, a rather small value compatible with the previous analysis [26], suggesting the high degree of crowding of the fullerene molecules. Indeed, the observed arrangement of the fullerene molecules allows a dense packing between the {0 0 1} planes, where the interfullerene mean distances are lower than 9.9 Å. In this arrangement, neighbours C$_{60}$ face each other with hexagons, which lie on planes slightly tilted of ~10° with respect to the a and b axes connecting the molecular centres.

In order to gain further insight on the monoclinic Li$_{12}$C$_{60}$ ground structure, we considered a Bärnighausen tree, showing the structural relationships connecting the observed structure (hettotype) with the original fcc C$_{60}$ phase (aristotype), by means of group-subgroup relations (see Figure 3). Lowering the symmetry from Fm$\bar{3}$m (C$_{60}$ fcc plastic phase) to I4/mmm requires the removal of the three-fold axis (t3). The successive loss of the centered translational symmetry (k2) leads to the primitive tetragonal space group P4$_2$/mnm, while the further removal of the four-fold screw axis (t2) brings to Pnnm. From Pnnm, the observed P2$_1$/c symmetry was reached by further removing a two-fold axis and a mirror (t2). All these intermediate orthorhombic space groups were checked as possible structural models of Li$_{12}$C$_{60}$ ground phase with MO-SA, but the constraints imposed by the symmetry operators to the molecular arrangement prevented from obtaining a good fit of the observed diffraction intensities.

In particular, the structure solution achieved in the space group P4$_2$/mnm leads to a molecular arrangement in which C$_{60}$s are statically disordered, due to the presence of the 4$_2$ symmetry element, incompatible with the C$_{60}$ icosahedral symmetry. On the other hand, MO-SA with Pnnm model gives similarly unsuccessful result, due to the constrained single degree rotational order of the molecules, not matching the observed pattern profile (see Figure 3).

The complete description of Li$_{12}$C$_{60}$ structure was obtained by localising Li atoms in the fullerene lattice interstices. Because of the unfavourable Li neutron scattering cross-section ($\sigma_{coe.} = 0.45$ barn, $\sigma_{inc.} = 0.92$ barn, $\sigma_{abs.} = 70.5$ barn, relative to natural Li isotopic abundance), as compared to carbon ($\sigma_{coe.} = 5.551$ barn, $\sigma_{inc.} = 0.001$ barn, $\sigma_{abs.} = 0.0035$ barn), the contribution of the intercalants to the structure factors is small, making this task quite challenging. Nevertheless, a good starting point was provided by the evaluation of the accessible surface in the carbon backbone for a sphere matching the Li ionic radius (0.68 Å). This allowed us to identify the presence of two different empty volumes in the fullerene structure, corresponding respectively to the pseudo-tetrahedral (smaller) and the pseudo-octahedral (bigger) voids of the parent cubic lattice, which are the best candidates to accommodate the alkali atoms. Further Rietveld refinement was performed inserting Li ions in the centre of the tetrahedral site (T), position 4e (1/2 0 1/4), in the centre of the octahedral site (O), position 2c (0 0 1/2) and in four non-distinctive (M) 4e positions (x y z), located around the octahedral centre and chosen in order to best fill the accessible solvent volumes detected (see Figure 1S). The refinement clearly improved by imposing a null occupation for the O position and a full one for the T position, while the Li in M positions tend to go away from the centre of the octahedral void; the best agreement was reached with a nominal stoichiometry Li$_{10}$C$_{60}$ ($R_{wp} = 6.01\%$, $R_{F2} = 3.17\%$) (see Tab. 1S). If one considers the pseudo-cubic representation for the fullerene molecules, Li ions were found to form clusters centred on the pseudo-tetrahedral interstices (Figure 4a): inside these clusters, the shorter Li–Li contact turn out to be ~2.7 Å, slightly shorter than in Li metal (3.0 Å at RT) and comparable to Li–Li distance in a ionic compound (2.54 ÷ 2.92 Å). This is in very good agreement also with the Li–Li distance found in the Li cluster in Li$_{12}$C$_{60}$ at high temperature [26], suggesting that the alkali atoms in the cluster are partially ionised.

Micro-Raman spectroscopy at room temperature was performed to better evaluate the entity of the charge transfer between the Li cluster and the C$_{60}$ molecule in Li$_{12}$C$_{60}$, by monitoring the A$_g$(2) pentagonal pinch-mode ('breathing mode') peak shift, which is proportional to the number of electrons donated to C$_{60}$. Undoped C$_{60}$ shows the A$_g$(2) at 1469 cm^{-1}, while an energy downshift of the peak of 6–7 cm^{-1} is expected for each electron transferred on C$_{60}$$^{n-}$ anion [28]. The spectrum collected in the energy window

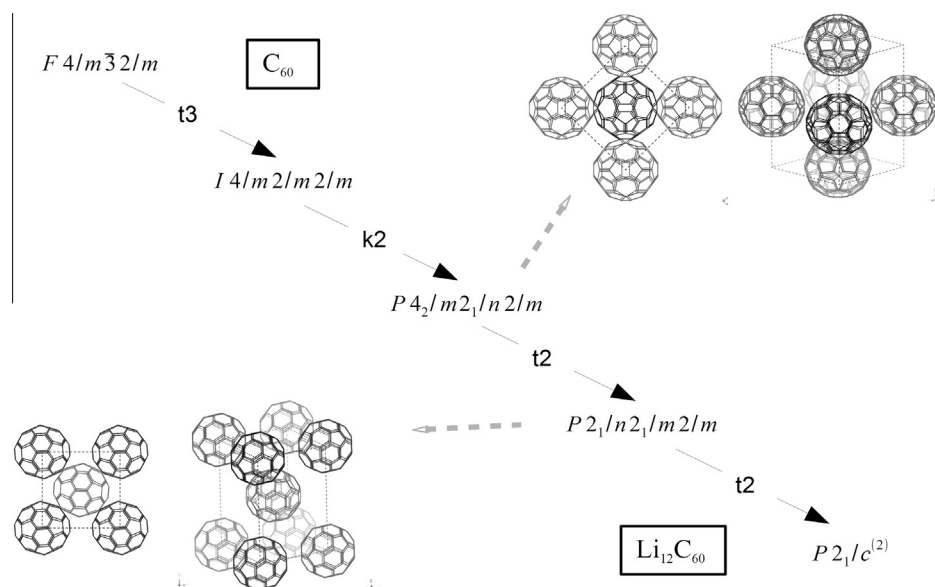**Figure 3.** Bärnighausen tree obtained using group-subgroup relation from the space group Fm$\bar{3}$m, of pristine C$_{60}$, to P2$_1$/n, observed in Li$_{12}$C$_{60}$.
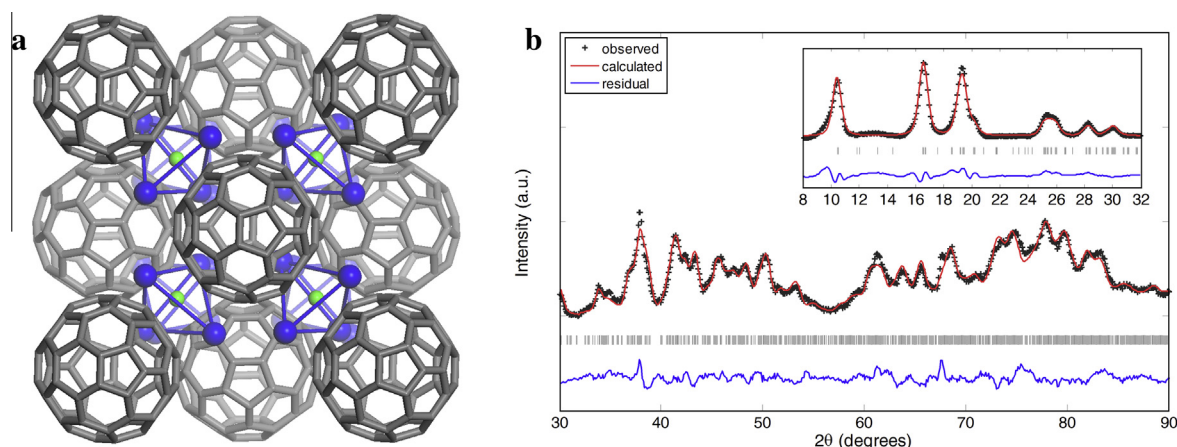
Figure 4. Localization of Li atoms in the $Li_{12}C_{60}$ structure. (a) Structure of Li clusters in $Li_{12}C_{60}$ showed in the parent cubic representation. (b) Final Rietveld refinement against the neutron diffraction data (R_{wp} = 6.01%, R_{F2} = 3.17%): the observed diffraction pattern was drawn with crosses, the calculated ones with the solid superimposing line, while differences are shown in solid line at the bottom. Vertical lines mark the reflection positions.

1100–1800 cm^{-1} (see Figure 5) shows the presence of the Raman modes expected for fullerenes in monomer state, indicating that no photo-polymerisation occurred during measurements. Several measurements, taken at different positions on the polycrystalline sample, sealed in a glass capillary, showed essentially the same result, thus confirming good sample homogeneity. The $A_g(2)$ peak energy downshift with respect pure C_{60} was estimated to be $\sim$40 cm^{-1}, being compatible with $\sim$6 electrons accepted by the fullerene during the solid state reaction with the alkali metal. This fact confirmed a partial charge transfer resulting from the intercalated Li, while part of the charge still reside on Li clusters.

The presence of an incompletely ionised cluster intercalated in the fullerite structure, together with the high negatively charged state of C_{60}, has proved to be of paramount importance in order to catalytically decrease the energy barrier required for the dissociation of the H_2 molecules [24] and to allow the hydrogen absorption mechanism, via the formation of $C_{60}H_y$. This process occurs at much lower temperatures in alkali doped fullerenes, as compared to pure C_{60} and is fully reversible [10,11]. In $Li_{12}C_{60}$, the presence of Li clusters appears particularly effective in this sense, leading to the onset of H_2 absorption already below 100 °C and an

uptake of 4.5 wt% of H_2 at 225 °C and 190 bar [12]. The present study indicated that Li clusters are located inside the smaller tetrahedral voids of the parent *fcc* structure, letting the bigger octahedral voids essentially unoccupied. However, the not complete stoichiometry detected by diffraction suggests that some Li ions do not participate to the clusters formation, but are probably disordered in the empty fullerene interstices. This fact is supported also by preliminary transport measurements, still in progress, indicating the presence of ionic contribution in the conductivity behaviour of $Li_{12}C_{60}$ already at low temperature and hence suggesting also a high Li mobility in this compound.

4. Conclusion

We managed to synthesize $Li_{12}C_{60}$ single-phase samples via a new direct and efficient solid-state technique, based on high energy ball-milling. *Ab-initio* structural investigation was performed using neutron powder diffraction data, which allowed us to understand the structure of the $Li_{12}C_{60}$ ground-phase. In this compound, fullerenes organise in a pseudo-cubic lattice described in the $P2_1/n$ space group with a peculiar arrangement, which allows to maximise their crowding in the {001} planes, while keeping a monomer state. On the other hand, Li atoms were found to form clusters, located in the pseudo tetrahedral voids of parent *fcc* lattice, letting the centre of the bigger octahedral void unoccupied. Raman spectroscopy indicated that the charge transfer from Li to C_{60} is not complete in this compound, suggesting that the Li clusters could play a role in the H_2 ab/desorption mechanism in this compound.

Appendix A. Supplementary data

Supplementary data associated with this article can be found, in the online version, at http://dx.doi.org/10.1016/j.cplett.2014.06.036.
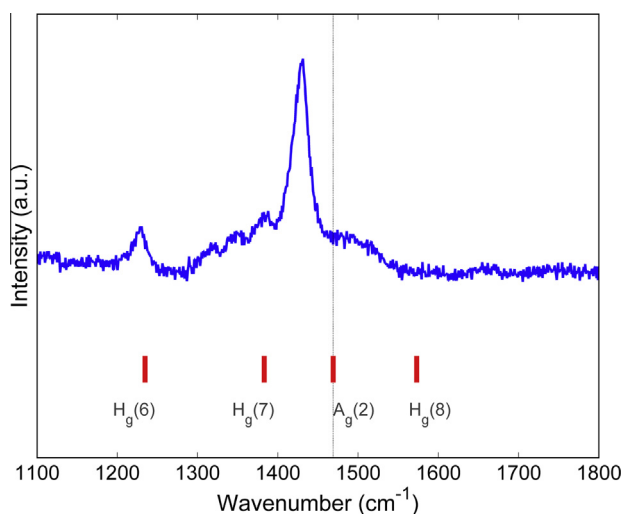

Figure 5. Raman spectrum of the $A_g(2)$ mode shows a shift from 1469 to 1429 cm^{-1} which corresponds to a charge transfer of 6 e^-. The vertical thicks mark the position of the Raman peaks in pristine C_{60}.

References

[1] L. Forró, L. Mihaly, Rep. Prog. Phys. 64 (5) (2001) 649.
[2] Y. Ihara et al., Phys. Rev. Lett. 104 (25) (2010) 256402.
[3] M. Riccò et al., Phys. Rev. B 72 (15) (2005) 155437.
[4] T. Wågberg, P. Stenmark, B. Sundqvist, J. Phys. Chem. Solids 65 (2–3) (2004) 317.
[5] P. Wzietek et al., Phys. Rev. Lett. 112 (6) (2014) 066401.
[6] M. Riccò et al., Phys. Rev. Lett. 102 (14) (2009) 145901.
[7] D. Pontiroli et al., Carbon 51 (2013) 143.
[8] B. Sundqvist, M. Yao, T. Wågberg, High Pressure Res. 28 (4) (2008) 597.
[9] B. Sundqvist, T. Wågberg, M. Yao, Diamond Relat. Mater. 20 (4) (2011) 600.
[10] J.A. Teprovich et al., Nano Lett. 12 (2) (2011) 582.
[11] P. Mauron et al., Int. J. Hydrogen Energy 37 (19) (2012) 14307.
[12] P. Mauron et al., J. Phys. Chem. C 117 (44) (2013) 22598.
[13] M. Aramini et al., Int. J. Hydrogen Energy 39 (5) (2014) 2124.
[14] D. Pontiroli et al., Fullerenes, Nanotubes, Carbon Nanostruct. 14 (2–3) (2006) 391.
[15] M. Yasukawa, S. Yamanaka, Chem. Phys. Lett. 341 (5–6) (2001) 467.
[16] S. Margadonna et al., J. Am. Chem. Soc. 126 (46) (2004) 15032.
[17] S. Margadonna et al., J. Am. Chem. Soc. 121 (26) (1999) 6318.
[18] M. Tomaselli et al., Phys. Rev. B 63 (11) (2001) 113405.
[19] M. Riccò et al., Phys. Rev. B 75 (8) (2007) 081401.
[20] D. Arčon et al., New J. Phys. 10 (3) (2008) 033021.
[21] J. Kohanoff, W. Andreoni, M. Parrinello, Chem. Phys. Lett. 198 (5) (1992) 472.
[22] Q. Sun et al., J. Am. Chem. Soc. 128 (30) (2006) 9741.
[23] T.P. Martin et al., J. Chem. Phys. 99 (5) (1993) 4210.
[24] M. Aramini et al., Carbon 67 (2014) 92.
[25] D.V. Schur et al., Carbon 41 (7) (2003) 1331.
[26] L. Cristofolini, M. Riccò, R. De Renzi, Phys. Rev. B 59 (13) (1999) 8343.
[27] T. Yildirim et al., Nature 360 (6404) (1992) 568.
[28] M.S. Dresselhaus, G. Dresselhaus, P.C. Eklund, J. Raman Spectrosc. 27 (3–4) (1996) 351.